STUDIES OF CREEP CRACK GROWTH UNDER HISTORY-DEPENDENT LOADING

F.W. BRUST
BATTELLE, Columbus, Ohio USA
B.S. MAJUMDAR
CIES Incorporated, Dayton, Ohio USA

ABSTRACT

The effects of load history on the creep crack growth process are discussed. There are three aspects of this problem which are considered: (i) The constitutive response of materials undergoing history dependent creep straining, (ii) the corresponding crack growth behavior including a discussion of fracture parameters capable of predicting the response, and (iii) experimental evidence of the importance of history dependent response. Finally, numerical studies which use the constitutive model and fracture theory of (i) and (ii) respectively are used to examine the experimental results developed in (iii).

KEYWORDS

Creep, Creep Crack Growth, Finite Element, Experimental, Fracture Mechanics, Time Dependent

INTRODUCTION

Most studies of creep crack growth to date have been concerned with simplified load conditions and constitutive relations. For constant load creep crack growth, the engineering approaches attempt to correlate crack growth rates with a parameter (i.e., C^*, C_t, K, etc.) (See References [1-5] for instance.) Simple creep-fatigue engineering approaches rely on Miner's Rule where the effects of creep crack growth and fatigue are considered separately. The correlating parameters for the engineering approaches rely on simple constitutive models such as Norton's or Strain Hardening Creep laws.

The approaches described above can provide useful engineering predictions of creep crack growth. However, for structural components which operate in a severe thermal environment, including the effects of thermal load history in the analysis procedure is essential for accurate crack growth predictions.

The development of a successful predictive analytical methodology involves (i) the choice of an appropriate constitutive model that incorporates both nonlinear material behavior and load history effects, and (ii) selection of a suitable fracture parameter that characterizes the crack tip process under constant and variable loads. Additionally, experimental data are generated that not only illustrate the importance of history dependence on creep crack growth, but also are used to verify the predictive ability of the analytical methods that are developed. This paper provides both experimental and computational results which illustrate the effects of load history on creep crack growth.

HISTORY DEPENDENCE

Uniaxial Bar. Fig. 1 illustrates the material response of a creeping solid which experiences stress reversals. Fig. 1a illustrates a uniaxial bar which is loaded, unloaded at t_1 and held, reloaded to σ at t_2 and held until time = t_3, then finally unloaded and held at negative stress. Fig. 1b illustrates the total creep strain which develops at as a function of time. Note that after each stress reversal, the creep strain increases rapidly for a period of time. Also shown in Fig. 1b are the corresponding strain-versus-time responses for the constant load case and when assuming classical strain hardening theory of creep. Fig. 1c shows the corresponding strain rate versus time response. Note that after each stress reversal, the strain rate increases rapidly. Note also from Fig. 1b that the strains predicted using classical strain hardening theory greatly underpredict the response. This process can be explained in terms of dislocations losing their mobility due to their piling up to obstacles and corresponding remobilization during stress reversals (See References [6, 7]).

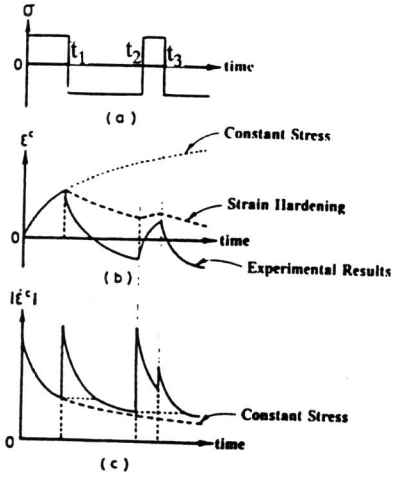

Figure 1. Creep Response Under Stress Reversals.

Crack Problem. Let us now focus on the corresponding crack problem. Creep strains develop and grow from the crack tip during the load hold period. Upon removal of the load, stress reversal occurs almost immediately at the crack tip because of the localized creep strains previously developed at the crack tip. When the load is completely removed, even to zero load (non-negative global load), a zone of compressive stresses which can be quite significant in size will develop. After reloading and subsequent hold, a zone near the crack tip experiences stress reversal again. Based on the discussions in the previous paragraph, it is seen that a zone in the crack tip region is continuously experiencing stress reversals and, correspondingly, increased strain rates and creep- damage. (An example is provided in the next section which illustrates this effect.) It is seen that, neglecting these reversals by using strain hardening theory may be quite non-conservative (Fig. 1b). For constant load problems, classical strain hardening theory and/or Norton Creep can be adequate for practical applications [3,5].

Constitutive Law and Performance for Crack Problems. A number of constitutive models have been proposed to predict high-temperature material response. However, their mathematical structures are often complicated and thus cumbersome to be employed in numerical analyses of creep behavior in cracked bodies. The determination of material constants in these models also causes major difficulties. One model that successfully describes creep under non-steady state of stress and for which material constants can be obtained very easily is that developed by Murakami and Ohno (7) and is based on the concept of a creep hardening surface.

This model has been shown to perform very well when compared to complex-load experimental data (Inoue et al. [8]). Moreover, in the Inoue benchmark problem (Inoue et al. [8], the Murakami and Ohno model performs as well or better than the ten other constitutive laws studied in that work.

Example - Crack Problem. Consider a standard compact tension specimen with crack length, a = 23.75 mm, uncracked ligament length, c = 27.05 mm. A finite element analysis of this specimen (9 CrMo Steel) was made with an imposed load spectrum consisting of : (1) Load with 24-hour hold period, (2) unload (to zero load), and hold for one hour, (3) reload and hold for 24 hours, and (4) etc. This spectrum was applied up to 99 total hours. This means that the end of the load-hold periods were 24, 49, 74, and 99 hours while the end of the unload-hold periods was 25, 50, and 75 hours (4 load and 3 unload periods). The specimen is made of 9 CrMo steel (at 538 C) with time hardening creep law:

$$\dot{\epsilon}^c = A\,\sigma^n\,t^m \qquad (1)$$

with

$$A = 7.09 \times 10^{-17},\ n = 5.6,\ m = 0.24$$

for stress in MPa and time in hours. These same constants are used for a strain hardening law and for the Murakami-Ohno cyclic creep law [7]. The Murakami-Ohno law can model the effects illustrated in Fig. 1 quite well.

The symmetric finite element mesh was a focused mesh with 10 rings of 6-noded isoparametric triangular elements surrounding the crack tip and 8-noded elements elsewhere. The element size at the crack tip is about 0.0005 c, which is about two and one-half times more refined compared to the mesh used by Shih and German [9] in their studies of HRR field dominance. Fig. 2a shows the y-direction (i.e., in the load direction) stresses directly ahead of the crack tip (along the symmetry plane). Fig. 2b shows the corresponding creep strains. For both stresses and strains, the importance of adequately modeling creep strains using the Murakami-Ohno creep law is evident.

Two interesting observations can be made regarding Fig. 2. The stresses tend to be higher when using a strain hardening law compared to the Murakami-Ohno law, while the creep strains are lower. This can be explained as follows. During the load changes (Fig. 1), the creep strain rates are greatly under-predicted using a strain hardening law while they are adequately predicted using the Murakami-Ohno law. Because of this, the stresses do not relax after load path changes as much as they should using a strain hardening law. At the same time, the corresponding creep strains do not accumulate as rapidly as they should using strain hardening theory. Interestingly, if the Murakami-Ohno results of Fig. 2a are examined on a log-log scale, the slope is about 0.15, which is what one expects for a constant load problem using a primary creep law $\frac{1}{n+1}$ (see Riedel [5]). More asymptotic studies will appear in upcoming publications. $R=0$

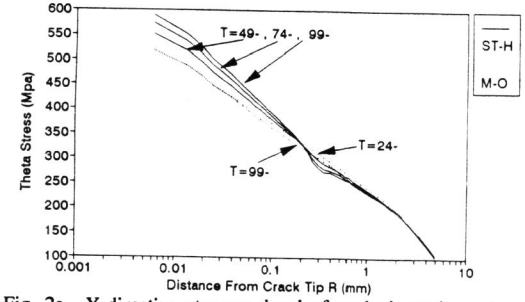

Fig. 2a. Y-direction stresses ahead of crack tip at the end of hold periods of 24, 49, 74, and 99 hours. M-O = Murakami-Ohno and ST-H = strain hardening.

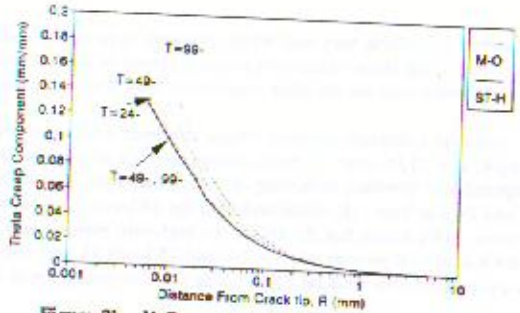

Figure 2b. Y-Component Total Creep Strains.

Fracture Parameters. Making a choice as to which fracture parameter(s) to focus on when attempting to characterize history dependent creep crack growth is difficult. We have placed different approaches into three categories: asymptotic approaches, damage or local approaches, and energetic or integral approaches.

Asymptotic approaches, wherein one develops the asymptotic solution to the crack problem for the situation of interest (elastic, plastic, creep, etc.) and fracture criterion is based on the strength of that field, work quite well for monotonically loaded problems. However, for history dependent loading, the asymptotic field may change during each cycle. Such fields are also known to change during crack growth. Moreover, the asymptotic field itself depends strongly on the constitutive law chosen. Hence, it is concluded that asymptotic approaches are impractical for characterizing history dependent fracture other than in an engineering sense.

Local approaches (Reference [10] are quite useful for predicting crack nucleation for all types of damage, including creep. For crack problems, however, there appears to be a problem. The procedure for both coupled or uncoupled damage theories consists of (i) developing the critical material parameter (scaler or tensor) D_c, (ii) determine a critical length parameter, l_c, i.e., the degree of the finite element refinement near the crack tip, so that experimental behavior is predicted. This same critical dimension is required for all other analyses. Because damage localizes at the crack tip, one finds that predicted results become more and more conservative as the mesh becomes more refined. This is because the finer the mesh, the greater the stress and strain gradients near the crack tip become and the more rapidly damage accumulates. The need for this critical-length parameter appears to render such methods insufficiently general to extend their use to history dependent creep damage.

Integral parameters have shown promise in several non-linear applications. A number of crack tip parameters expressed in integral forms have appeared in the literature. These include Blackburn [11] (J_B); Kishimoto, Aoki, and Sakata [12] $\hat{J}$; McClintock [13] (J_M); Watanabe [14] (J_W), Brust and Atluri [15] (T), and Cherepanov [16]; and others.

The physical interpretation of many of these integral parameters is not entirely clear except for the T^*. Brust, Nakagaki, and Gilles [17] showed that the physical interpretation of the T^* integral is that of the energy release rate to a finite-sized material volume in the vicinity of the crack tip. NASA Lewis (and their engine subcontractors) have experienced great success in attempting to use integral parameters to characterize high-temperature severe load (creep-fatigue) conditions (Kim et al. [18]). In this paper we also examine the use of these integral parameters.

Experiments. Here we shown an example of the behavior of a compact-tension specimen made of a 9 Cr-1Mo steel which is subjected to the high-temperature (528 C) load spectrum illustrated in Fig. 3. The experimental technique is automated with details presented in References [19, 20]. The five-minute hold time was enough time for significant displacement recovery to occur. Crack growth began at about the eighth day. An example of the load-point displacement and crack-growth response (crack growth is related to EP) is provided in Figure 4a for days 25 to 28. Note that after each unload/reload, the displacement rates increase compared to the previous unload/reload period. In addition, the displacement

immediately after reloading is smaller than the value before unloading. This occurs because of displacement recovery as the compressive stresses develop at the crack tip. Fig. 4b illustrates the detailed load displacement response at the 27th day. Again, observe the displacement recovery during the unload cycle. After reload, the initial displacement is smaller than the value before unloading. With time, the displacement eventually overtakes the value before unloading.

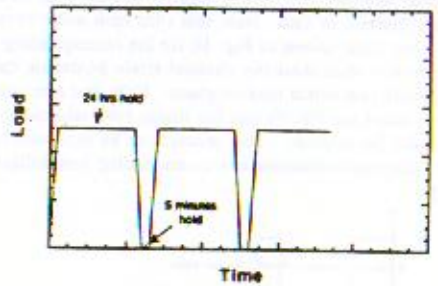

Fig. 3. Load Spectrum for 9CR-1Mo Test

From Figs. 4a and 4b it is clear that the unload cycles, even to zero load, increase the displacement rates compared to constant load tests. The displacement rates of Fig. 4 would be a constant value during days 25 to 28 if unloading had not occurred. The global load vs. displacement behavior experiences a hysteresis loop as seen in Fig. 4b. Indeed, near the crack tip, the stress strain hysteresis loops are much greater.

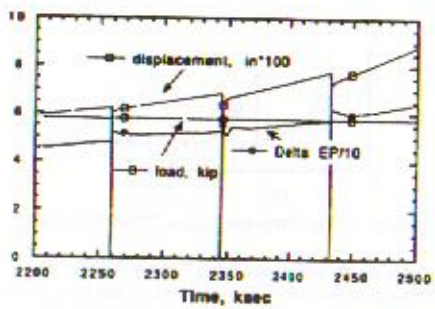

Fig. 4a. Details of Displacement Response Between Days 25 to 28 For 9CR-1Mo Test

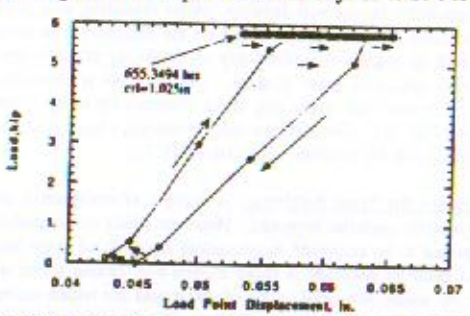

Fig. 4b. Detailed Load Displacement Response During The 27-Day Cycle

ANALYSIS RESULTS

History Dependent Load. The load history shown in Fig. 3 was modeled, with results compared to the experimental data. The applied load was 23.353 KN and plane stress was assumed. The predicted and experimental displacements throughout the entire 700 hours considered here are shown in Fig. 5. The analysis used the Murakami-Ohno constitutive law. Predictions using either the Norton or strain-hardening creep law only are significantly lower than these. The upper curve represents the experimental and predicted displacements at the end of the hold period, just before unloading, while the lower data points represent the displacements at the end of the unload period. The comparison is reasonable except beyond about 630 hours, where the predicted results begin to become large. The experiment began to experience unstable behavior at times greater than 700 hours.

Fig. 5b shows an enlargement of the experimental and analysis displacements between the times of 360 to 460 hours. The displacement recovery upon unload, the corresponding reduced displacement (compared to before unload) after reloading, and the increased displacement rates after the cycle are evident. This same effect is observed experimentally with the effect becoming more important when crack growth is occurring (see Reference [20] and Fig. 4a. A further enlargement of these comparisons is shown in Fig. 5b near the time of 438 hours. Note that the relative trends between the analysis and experiment are very close while the magnitudes vary somewhat. The displacement recovery after un. .i is seen here.

Fig. 6a compares all of the integral parameters as a function of time. The T^* and J_W integrals both experience a step jump after each cycle, as expected. The J_B, $\hat{J}$, and J_M integrals also do, but to a much smaller extent. This makes the practical application of these less convenient. Note also that the J_M and $\hat{J}$ parameters are almost identical. This is because the W_e term in $\hat{J}$ is very small here.

As indicated in Fig. 6a, crack growth begins at 192 hours, after the eighth unloading. Note that, before crack growth, all integrals experience a step jump after unloading. Also, observe that the experimental scheme of Fig. 3 is not strictly adhered to, as several times 48 hours elapsed, and, once, 72 hours, before an unload cycle. Also note that the T^* integral attains a nearly constant value (close to the nucleation value) throughout the entire time history (between 100 and 130 KJ/m^2, as indicated by the lines in Fig. 6a). This suggests that a constant value of T^* may characterize crack growth under creep fatigue conditions. The same comment applies to J_W. The resistance curves are plotted in Fig. 6b. The same lines are drawn between 100 and 130 KJ/m^2 to compare. After about 628 hours the curves become unstable, suggesting that unstable creep failure is predicted.

The nearly constant values for T^* and J_W during crack growth suggest that these parameters may be used as a creep fracture parameter for cyclic creep. The fact that they are not perfectly uniform is due to three-dimensional crack-growth effects and the plane-stress assumption. However, this suggests that these integrals may be used to predict crack initiation as well as growth by using the value at initiation throughout the history. Many more details are forthcoming in future publications.

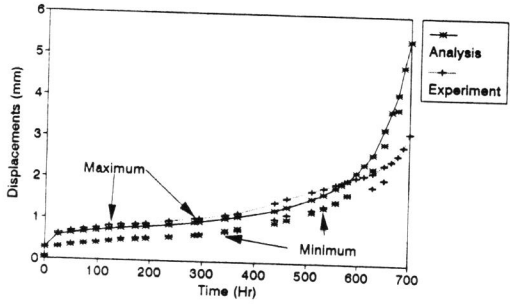

(a) Entire History

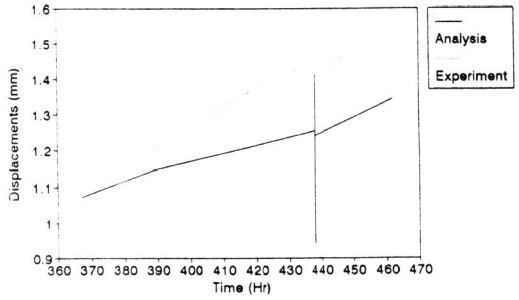

(b) Detail Between 360 And 460 Hours Including Unloading

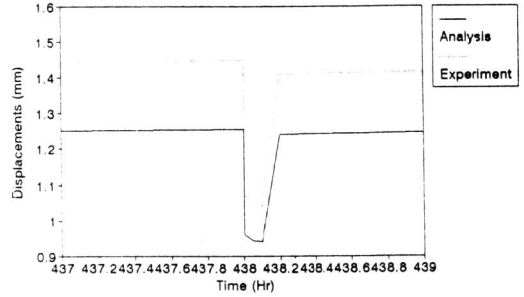

(c) Unload Detail At Time = 438 Hours

Fig. 5. Displacement Comparisons

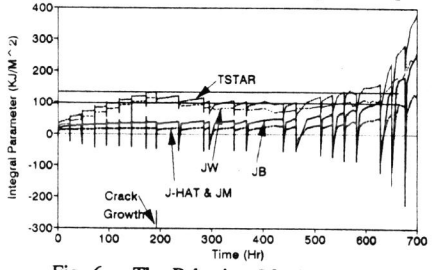

Fig. 6a. The Behavior Of All Integral Parameters Versus Time

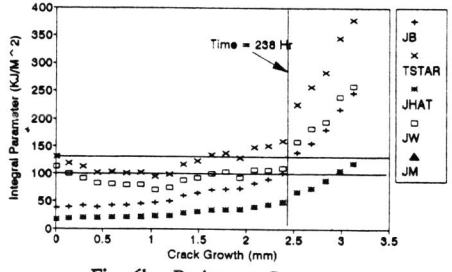

Fig. 6b. Resistance Curves

ACKNOWLEDGEMENT

This work was supported by the U.S. Department of Energy, Office of Basic Engineering Sciences, under Grant No. DE-FG02-90ER14135.

REFERENCES

[1] Sadananda, K. and Shahinian, P., "Review of the Fracture Mechanics Approach to Creep Crack Growth in Structural Alloys," Engineering Fracture Mechanics, Vol. 15, pp. 327-342, 1981.

[2] Landes, J. D. and Begley, J. A., in Mechanics of Crack Growth, ASTM STP 490, American Society for Testing and Materials, pp. 128-148, 1976.

[2] Landes, J. D. and Begley, J. A., in Mechanics of Crack Growth, ASTM STP 490, American Society for Testing and Materials, pp. 128-148, 1976.

[3] Saxena, A., "Creep Crack Growth In High Temperature Ductile Materials," Engineering Fracture Mechanics, Vol. 40, No. 415, pp. 721-736, 1991.

[4] Leung, C. P. and McDowell, D. L., "Inclusion of Primary Creep in the Estimation of the C_t Parameter," International Journal of Fracture, Vol. 46, pp. 81-104, 1990.

[5] Riedel, H., Fracture at High Temperatures, Springer-Verlag, 1987.

[6] Gittus, J., "Viscoelasticity and Creep Fracture in Solids," Applied Science, London (1975).

[7] Murakami, S., and Ohno, N., "A Constitutive Equation of Creep Based On The Concept Of A Creep Hardening Surface," Int. J. of Solids and Structures, Vol. 18, No. 67, pp. 597-609, 1982.

[8] Inoue, T., et al., "Evaluation of Inelastic Constitutive Models Under Plasticity-Creep Interaction Condition," Nuclear Engineering and Design, Vol. 126, pp. 1-11, 1991.

[9] Shih, C. F., and German, M. D., "Requirements For A One Parameter Characterization Of Crack Tip Fields By The HRR Singularity," International Journal of Fracture, Vol. 17, No. 1, February, 1981.

[10] Lemaitre, J., and Chaboche, J. L., "Mechanics of Solid Materials," Cambridge University Press, 1990.

[11] Blackburn, W. S., "Path Independent Integrals To Predict Onset of Crack Instability In An Elastic Plastic Material," Int. Journal of Fracture Mech., Vol. 8, pp. 343-346, 1972.

[12] Kishimoto, K., Aoki, S., and Sakata, M., "On The Path Independent Integral-J," Engineering Fracture Mechanics, Vol. 13, pp. 841-850, 1980.

[13] McClintock, F. A., in Fracture 3, Ed. H. Liebowitz, Academic Press, 1971.

[14] Watanabe, K., "The Conservation Law Related To Path Independent Integral And Expression Of Crack Energy Density By Path Independent Integral," Bul. of JSME, Vol. 28, No. 235, January 1985.

[15] Brust, F. W. and Atluri, S. N., "Studies On Creep Crack Growth Using The T* Integral," Engineering Fracture Mechanics, Vol. 23, No. 3, pp. 551-574, 1986.

[16] Cherepanov, G. P., "A Remark On The Dynamic Invariant Or Path-Independent Integral," Int. J. Solids and Structures, Vol. 25, No. 11, pp. 1267-1269, 1989.

[17] Brust, F. W., Nakagaki, M., and Gilles, P., "Comparison of Elastic-Plastic Fracture Mechanics Techniques," ASTM STP 1074, pp. 448-469, 1990.

[18] Kim, K. S., et al., "Elevated Temperature Crack Growth," Final Report to NASA Lewis Research Center, November, 1988.

[19] Brust, F. W., and Krishnaswamy, P., "A Computational Study of The Time Dependent Crack Growth Process," in ASME Applied Mechanics Division Volume (AMD), proc. of ASME 1992 Winter Annual Meeting, A. Nagar Ed., 1992.